Hydration Dependence of the Wood-Cell Wall Structure in *Picea abies*. A Small-Angle X-ray Scattering Study

H. F. Jakob,[†] S. E. Tschegg,[‡] and P. Fratzl*,[†]

Institut für Materialphysik der Universität Wien, Boltzmanngasse 5, A-1090 Wien, Austria, and Institut für Meteorologie und Physik der Universität für Bodenkultur, Türkenschanzstrasse 18, A-1180 Wien, Austria

Received April 17, 1996; Revised Manuscript Received July 29, 1996[⊗]

ABSTRACT: Hydration dependent structural changes at the nanometer level were investigated in the natural wood cell of *Picea abies*. Using the technique of small-angle X-ray scattering (SAXS), it was possible to investigate the same specimens at different degrees of hydration, x, in a nondestructive way, which allowed us to separate the scattering from pores from the scattering of the cell wall itself. For specimens dried below the fiber saturation point, x_F, the scattering from pores and other cavities dominated and considerable changes of the cell-wall structure occurred. In the native state (for $x > x_F$), however, the structure of the cell wall was independent of the hydration. The structure function describing the relative arrangement of the cellulose fibrils was obtained for the native cell wall. It was in quantitative agreement with the prediction from a hard-disk model with packing density 0.3, corresponding to a typical spacing between fibril centers of about 40 Å.

1. Introduction

Wood is a hygroscopic material which absorbs water molecules due to hydroxyl groups in its cell wall material.[1−4] The system wood−water is important in many fields of wood technology, mainly because a change in water content also changes the structure of wood on a macroscopic level and, therefore, its mechanical properties.[2,3] Usually, water in wood appears in three different forms:[2,3] as bound water in the cell wall and as free water or vapor in the voids and lumina. Water molecules are bound to free OH dipoles at the surface of the cellulose fibrils and inside the cell-wall matrix. The crystalline region of the elementary cellulose fibrils (ECF's), however, is inaccessible to water molecules because the OH groups are satisfied by the formation of hydrogen bonds between adjacent cellulose chains.

When water is absorbed into the cell wall, anisotropic swelling occurs and the relative increase of the linear dimension in radial, α_r, tangential, α_t, and longitudinal, α_l, direction of the stem satisfies[5] $\alpha_t > \alpha_r > \alpha_l$. The correlation between the specimen volume and the water content x is roughly linear,[2,6] up to the point where fiber saturation is reached. The fiber saturation point x_F is defined as the hydration where all chemical and physical binding sites for water molecules are saturated within the cell wall. For spruce wood, x_F varies between 30 and 34%.[2,7] At higher moisture contents, water is mainly absorbed as free water, predominantly within microvoids or capillaries. This condensation beyond the fiber saturation point does not cause further volume expansion.[3]

Trees grow in a water-saturated ($x > x_F$) environment and begin to lose their moisture content as soon as they are felled. While the macroscopic effects of the subsequent drying process are well documented,[2,3] the aim of the present paper is to investigate structural changes at the nanometer level, that is, at dimensions corresponding to the typical thickness of ECF's. The method used is small-angle X-ray scattering (SAXS), which is ideally suited to study the nanometric structure in a nondestructive way. Hence, it was possible to investigate the same specimens at different degrees of hydration. Previous experiments[8] have shown that the SAXS patterns from native wood of *Picea abies* can be regarded as arising from a two-phase composite, cellulose fibrils in a hemicellulose−lignin matrix, but with contributions from pores and other cavities at very small scattering angles. Hence, only the fibril diameter, but no information on the fibril packing, had been obtained in these earlier studies. The varying amount of water in the cavities at moistures above the fiber saturation point ($x > x_F$) was exploited here to separate the scattering from cavities and from the cell-wall material using a "contrast matching" procedure. The so-obtained scattering function from the cell wall of native *P. abies* (not contaminated by contributions from pores) was now used to extract information on the packing of cellulose fibrils. The results are compared quantitatively to the packing predicted by a model of hard disks. Finally, the effects on the cell-wall structure of drying below the saturation point ($x < x_F$) are also documented.

2. Materials and Methods

2.1. Specimen Preparation. Specimens were taken from a freshly felled spruce (*P. abies*) and immediately stored in liquid nitrogen, i.e. before any water desorption processes took place. To preserve the specimens in their natural condition, the slices were cut with a cryomicrotome at approximately −37 °C along the longitudinal direction of the tree. The slices were then stored in liquid nitrogen until the SAXS measurements were carried out. Tangential slices with a thickness of ∼200 mm were taken from the early wood part of an annual ring, where the elementary cellulose fibrils are known to be arranged in parallel arrays along the longitudinal direction of the stem.[8,9] For the scattering measurements neither chemical nor physical treatment of the specimens was necessary. As the samples were placed into the high-vacuum chamber of the X-ray apparatus, they were encapsulated in a plastic foil of 100 μm in total thickness in order to prevent drying. The degree of hydration of the sample was determined according to the formula

$$x = \frac{m_x - m_0}{m_0}$$

* To whom correspondence should be addressed (e-mail: fratzl@pap.univie.ac.at).
[†] Institut für Materialphysik der Universität Wien.
[‡] Institut für Meteorologie und Physik der Universität für Bodenkultur.
[⊗] Abstract published in *Advance ACS Abstracts,* October 1, 1996.

S0024-9297(96)00566-9 CCC: $12.00

where m_x is the weight of the sample at hydration x and m_0 its dry weight. Several samples were investigated at different moisture contents down to the vacuum dry state. The weight of the specimen was determined before and after each measurement during which it was encapsulated to prevent drying. In between two measurements, the humidity was reduced by keeping the specimen for some time on the scales at ambient condition. At low hydrations, dry air from a hairdryer, operated at low temperature, was used to decrease the humidity of the specimen. The dry weight was measured for all samples after drying for several hours in high vacuum at room temperature. The initial moisture content was the native state for most specimens, in some cases it was increased as much as possible by immersing the specimen in water. In this way, hydrations ranged from $x = 0$ up to $x = 250\%$.

For the SAXS measurements, the longitudinal direction of the samples (i.e. the direction of the stem axis) was perpendicular to the incoming X-ray beam. Scattering patterns were collected with a typical time of 0.5 h per measurement to provide sufficient counting statistics and corrected for transmission and instrumental background. The scattering intensity of the foil was practically negligible in the interesting range of scattering vectors.

2.2. Spherically Averaged SAXS Intensities. The scattering intensity $I(\vec{q})$ was collected as a function of the scattering vector $\vec{q}$ with modulus $q = |\vec{q}| = (4\pi/\lambda) \sin \theta$, where 2θ is the angle between the incoming and the scattered X-ray beam and λ the X-ray wavelength. The experimental setup consisted of a 12 kW rotating anode X-ray generator used in a point-focus geometry. The incoming X-ray beam had a circular cross-section of 0.6 mm in diameter. The radiation wavelength was $\lambda = 1.54$ Å, corresponding to Cu Kα radiation in combination with a Ni filter. The spectra were taken with a two-dimensional position sensitive detector (Fa. Siemens) with a sample to detector distance of 100 cm.

As we have shown in a previous work,[8] the scattering intensity arising from the elementary cellulose fibrils (ECF's) out of the S_2 cell-wall layer of early wood has practically cylindrical symmetry around the longitudinal axis of the stem. Hence, writing the scattering intensity in spherical coordinates (q,Ω), one gets

$$I(\vec{q}) = I(q,\Omega) = I(q,\varphi)$$

The solid angle Ω was defined over the two Eulerian angles $\Omega = (\chi,\varphi)$, with χ measured in the plane perpendicular to the symmetry axis. $I(\vec{q})$ does not depend on χ because of the cylindrical symmetry. The spherical average $\tilde{I}(q)$ of the intensity is defined by an integration over Ω:

$$\tilde{I}(q) = \frac{1}{4\pi}\int_\Omega I(q,\Omega)\, d\Omega = \frac{1}{2}\int_0^\pi d\varphi\, I(q,\varphi) \sin \varphi$$

because $d\Omega = \sin \varphi\, d\chi\, d\varphi$. A typical two-dimensional SAXS measurement of a tangential section of early wood, representing $I(q,\varphi)$, is shown in Figure 1a. The correction for $\sin \varphi$, i.e. $I(q,\varphi) \sin \varphi$, is shown in Figure 1b. As one can see, the streak in Figure 1a stays almost unchanged by this transformation, the main changes occurring around the (horizontal) cylindrical symmetry axis where $\sin \varphi$ differs significantly from 1.

In excellent agreement with previous measurements,[8,9] the spherically averaged intensity could be described in the region $q > 0.3$ Å^{-1} as $\tilde{I}(q) = \text{bgr} + (\text{const})(1/q)(2J_1(qR)/(qR))^2$, where J_1 is the Bessel function of the first kind and $R = 12.5$ Å for all specimens. For further treatment of our data, we subtracted the constant background (=bgr) from the spherical averages; i.e. we used transmission-normalized, background-corrected data $\tilde{I}(q)$. To account for the hydration dependence of $\tilde{I}(q)$, we also used the notation $\tilde{I}_x(q)$ for the integral intensity at hydration x.

3. Results

Figure 2 shows the dependence of $q\tilde{I}_x(q)$ upon varying hydration x, where $\tilde{I}_x(q)$ is the background-corrected, spherically averaged scattering intensity. For large values of q, this intensity is virtually independent of the hydration x (see Figure 2), as long as $x > x_F$ (≈30%). This is due to the fact that the scattering from pores

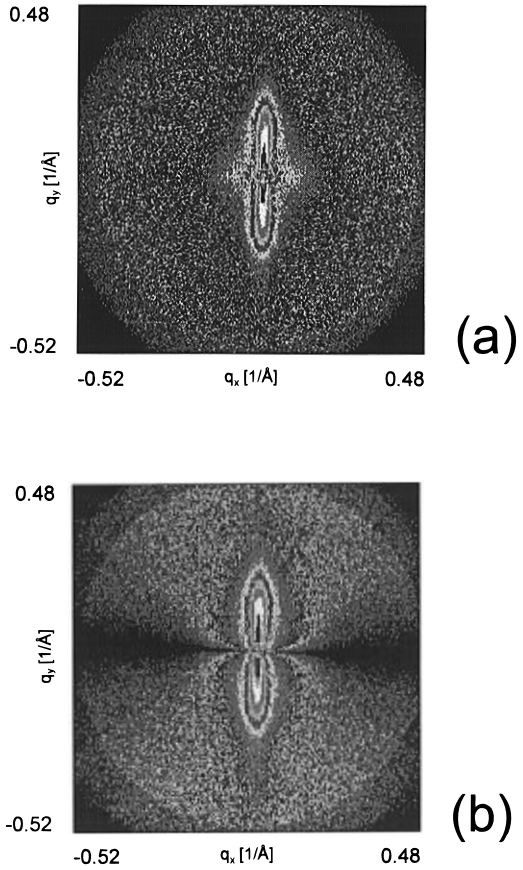

Figure 1. Two-dimensional SAXS measurements from a tangential section of *P. abies* displayed in a pseudogray scale. (a) The measured intensity $I(q,\varphi)$ is displayed and compared with the transformed intensity $I(q,\varphi) \sin \varphi$ shown in (b). We used patterns of the form shown in (b) to compute spherical averages of the SAXS intensities.

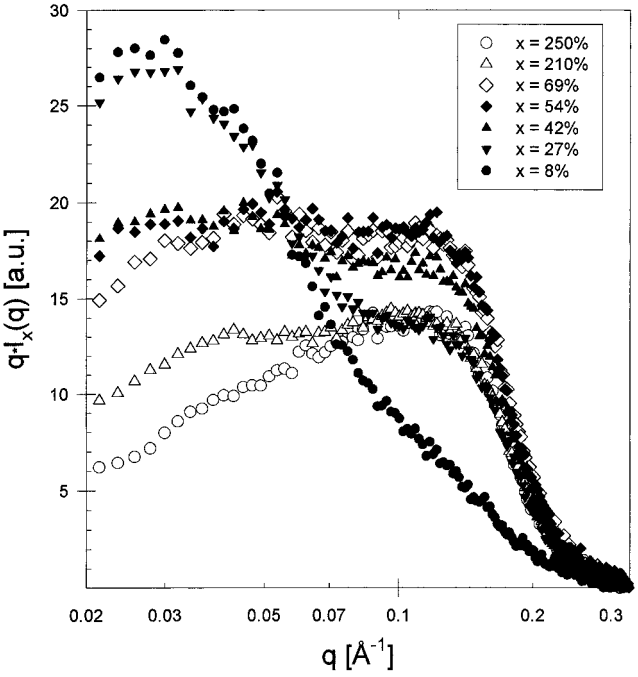

Figure 2. Spherical averages as obtained by a φ-integration of Figure 1b for several hydrations x. Shown are $q\tilde{I}_x(q)$, where $\tilde{I}_x(q)$ is the transmission and background corrected spherically averaged intensity, plotted versus the scattering length q.

and other cavities (which are large compared to the thickness of ECF's) only contribute at small q, while at large q one measures the scattering from the ECF's in the hemicellulose−lignin matrix. On the other hand, we observe a strong increase of the intensity with decreasing hydration at small q, where the scattering of pores and microvoids dominates. These observations suggest that the total scattering intensity can be regarded as the sum of a contribution from the cell wall (ECF's in the hemicellulose−lignin matrix) and from the pores and other cavities. This leads to the following expression for the spherically averaged intensity $\tilde{I}_x(q)$ at hydration x

$$\tilde{I}_x(q) = \frac{\pi}{q} I_x^{CW}(q) + I_x^{P}(q) \qquad \text{(A1)}$$

$I_x^{CW}(q)$ is the scattering intensity from a two-dimensional cross-section, perpendicular to the cellulose fibril direction of the S_2 layer of the cell wall. Taking into account the fact that cellulose fibrils are very elongated, practically cylindrical objects, the spherically averaged intensity is then given by $(\pi/q)I_x^{CW}(q)$.[10−12]

$I_x^{P}(q)$ is the scattering from pores and cavities. We further use the following approximations:

•For hydrations x larger than the fiber saturation point x_F, the cell wall is known to be saturated with water. Hence, its scattering can be supposed to be roughly independent of x. We take

$$I_x^{CW}(q) = \lambda(x)\, I^{CW}(q) \qquad (x > x_F) \qquad \text{(A2)}$$

where the constant $\lambda(x)$ varies only slightly (to account, e.g., for small variations in specimen thickness).

•The pores do not change their structure when they are emptied or filled with water.[3] Only their scattering contrast changes, as they are gradually filled with water, and

$$I_x^{P}(q) = \alpha(x)\, I^{P}(q) \qquad \text{(A3)}$$

•The scattering of pores and other cavities dominates at very small values of q ($q < 0.03$ Å^{-1}). Indeed, this is indicated by the large variation with x of the intensity at $q = 0.02$ Å^{-1} (see Figure 2) and the fact that $I_x^{CW}(q)$ does practically not change with x for $x > x_F$ (see eq A2). In other words we assume the scattering intensity to be

$$\tilde{I}_x(q) \approx I_x^{P}(q) \qquad (\text{for } q < 0.03 \text{ Å}^{-1}) \qquad \text{(A4)}$$

According to these hypotheses, first the parameter $\alpha(x)$ was determined by normalizing all intensity functions $\tilde{I}_x(q)$ to the same average value at $0.02 < q < 0.03$ Å^{-1}. Then, for all hydrations $x > x_F$, the normalized intensities

$$\frac{1}{\alpha(x)}\tilde{I}_x(q) = I^{P}(q) + \frac{\lambda(x)}{\alpha(x)}\frac{\pi}{q} I^{CW}(q)$$

were plotted as functions of q. Subtracting two such curves for different x eliminates $I^P(q)$ and allows the determination of a function proportional to $I^{CW}(q)$. Using this function and the expression above, a simultaneous fit of all data for $x > x_F$ (see Figure 3) gave an estimate for $I^P(q)$ and the values of λ/α as a function of x. Figure 4 shows a plot of $I^P(q)$ versus q. For q larger than about 0.1 Å^{-1}, the scattering from pores turned out to be so small compared to the scattering from the cell wall that $I^P(q)$ could not be determined with accurate statistics. Between $0.03 < q < 0.1$ Å^{-1}, the data points in Figure 4 can be reasonably described by a power law $I^P(q) \propto q^{-4}$. In agreement with Porod's law,[13] this indicates sharp interfaces between the cavities and cell-wall substances. Hence, $I^P(q)$ was fitted with a Porod's law in the interval $0.03 < q < 0.1$ Å^{-1}

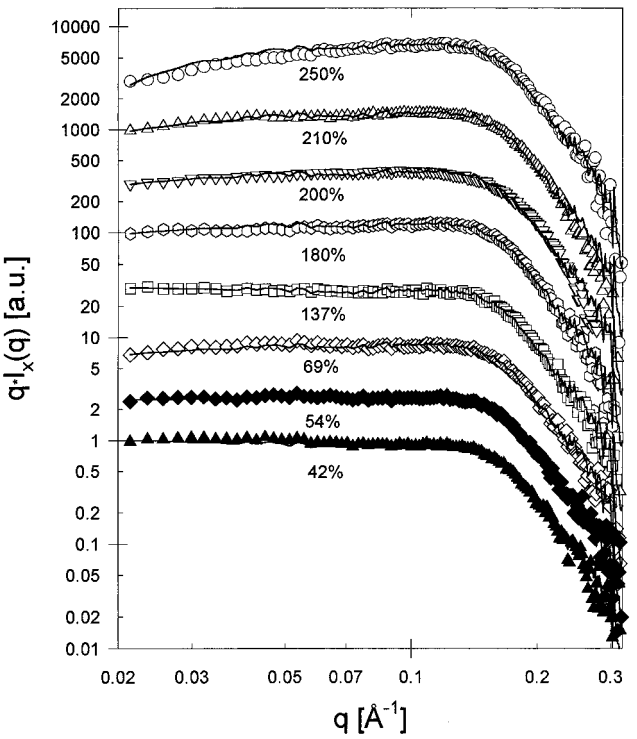

Figure 3. Scattering intensities $q\tilde{I}_x(q)$ displayed on a double-logarithmic scale as a function of q. The curves were shifted by an arbitrary amount along the axis of ordinates to avoid superposition of the data. The solid lines represent fits of the measured intensities using the two functions $I^P(q)$, and $I^{CW}(q)$ and the numbers $\lambda(x)/\alpha(x)$ for each hydration x (the values of x are indicated in the figure).

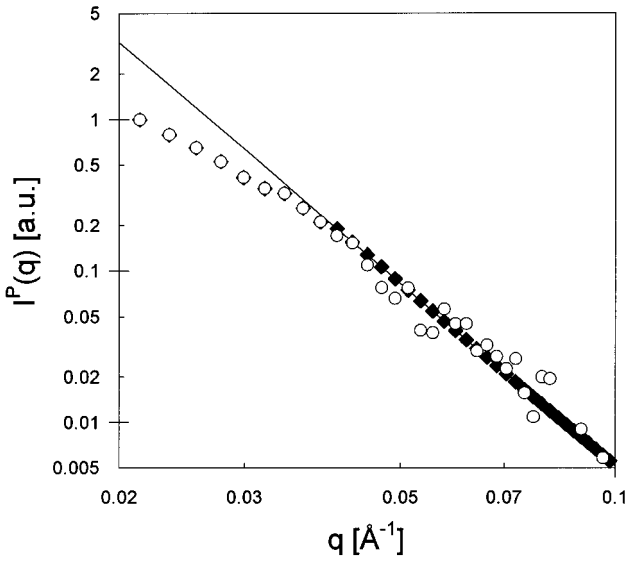

Figure 4. Scattering function from pores and lumina $I^P(q)$ within the wood specimen. The white circles correspond to the measured data, and the solid line represents a best fit for $0.03 < q < 0.1$ Å^{-1} using Porod's law. In the region $q > 0.03$ Å^{-1} the measured data points were replaced by the estimate from Porod's law (diamonds).

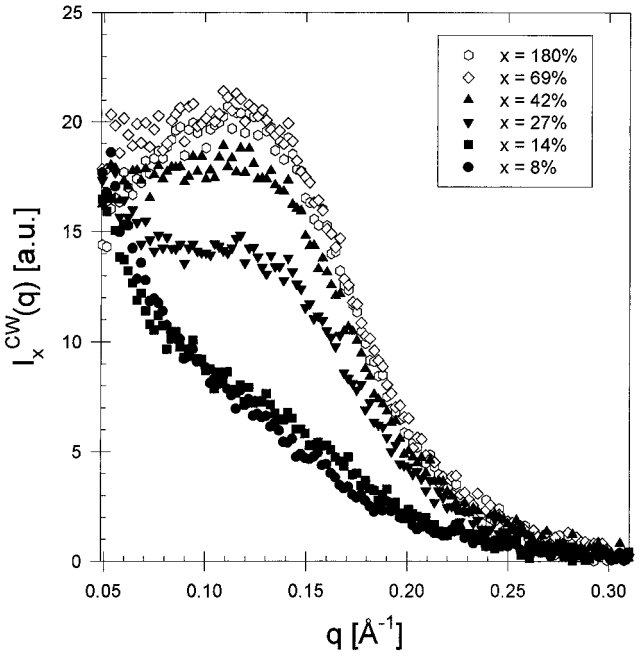

Figure 5. Scattering function $I_x^{CW}(q)$ from the cell wall only, for several water contents x of the specimen.

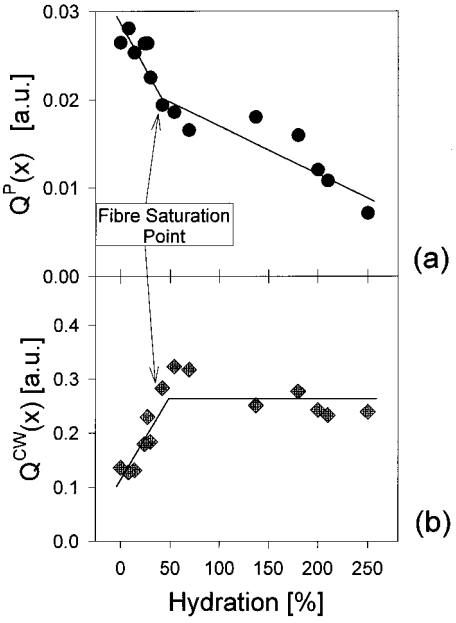

Figure 6. Integral intensity of the scattering from pores (a) and from the cell wall (b) as a function of the hydration x.

and extrapolated to large q with this analytical expression (see Figure 4).

Combining the assumptions A1 and A3 with the values for $\alpha(x)$, determined above (using assumption A2), and the scattering curve from the pores, given in Figure 4, it was possible to plot the scattering from the cell wall only. This is shown in Figure 5 for different hydrations above and also below the saturation point x_F. As one can see, there are enormous structural changes up to a hydration of $x = x_F$, while the curves become virtually identical for $x \geq x_F$.

To estimate the x dependence of the proportion of scattering from pores and from the cell-wall substances, we further calculated the integral intensities

$$Q^P(x) = \alpha(x) \int I^P(q)\, q^2\, dq$$

and

$$Q^{CW}(x) = \pi \int I_x^{CW}(q)\, q\, dq$$

respectively, and displayed them versus the hydration x in Figure 6.

Finally, information on the arrangement of cellulose fibrils within the native cell wall may be gained in the form of a structure function $G(q)$. Indeed, if cellulose fibrils are approximated by cylinders of diameter D = 2.5 nm,[9] they will appear as disks in a planar cross-section through the cell wall along a plane perpendicular to the fibril direction. The structure function $G(q)$ describing the correlation between the centers of those disks can then be obtained from the formula[11]

$$I^{CW}(q) \propto F(q)\, G(q)$$

where $F(q) = (2J_1(D/2q)/(Dq))^2$ is the form function of the disks and J_1 the Bessel function of the first kind. The scattering signal from the native wood-cell wall, $I^{CW}(q)$, is plotted in Figure 7a. The resulting structure function, $G(q)$, shown in Figure 7b, has a distinct maximum in the region around q = 0.15 Å^{-1} and oscillates around 1 at larger q. This indicates that within the planar cross-section perpendicular to the fibril direction, the centers of ECF's are typically

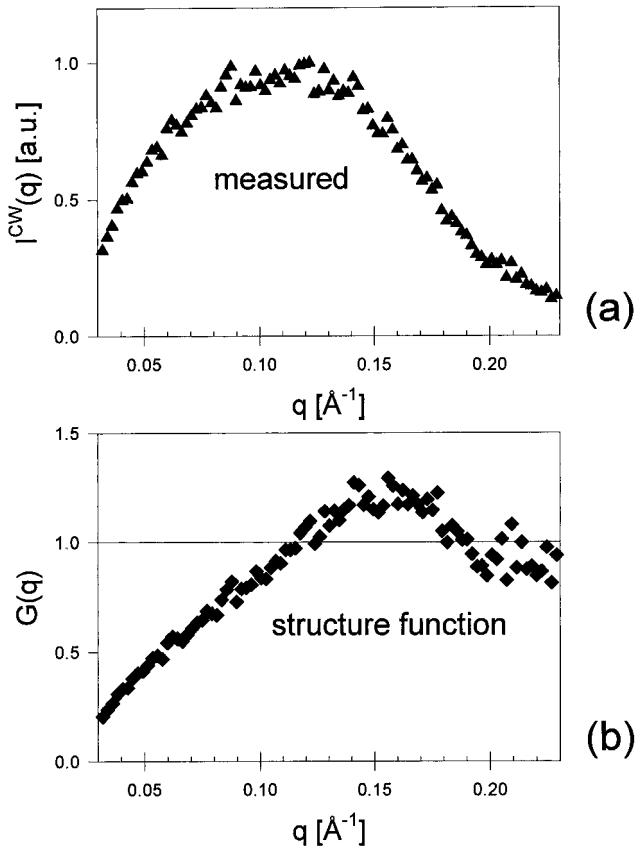

Figure 7. (a) Scattering function $I^{CW}(q)$ from the water-saturated cell wall and (b) the structure function $G(q)$. $G(q)$ was normalized by an arbitrary factor.

separated by a distance $\approx 2\pi/0.15$ = 42 Å, which is somewhat larger than the diameter of the disks of 25 Å.

4. Discussion

The SAXS measurement of tangential wood sections at various degrees of hydration allowed the extraction of the scattering from pores (Figure 4) and from the cell wall (Figure 5), separately. The integral intensity of

these two components, shown in Figure 6, characterizes the relative importance of the contributions. In particular, it is clearly visible that the contribution from pores $Q^P(x)$ becomes negligible with respect to the scattering from the cell wall $Q^{CW}(x)$ at sufficiently high water content x. For dry specimens ($x < x_F$), the pore contribution dominates. It is also remarkable that the curves for both Figure 6a,b show a bend at the same hydration, namely the fiber saturation point x_F.

Figure 6a shows that the scattering from pores decreases continuously with increasing x, corresponding to the fact that the contrast between pores and the cell-wall substances is reduced when the voids are filled with water.

In Figure 6b one can see, as described in the previous sections, that the scattering from cell-wall substances virtually stays constant, when x diminishes to x_F. This is due to the fact that the cell wall properties remain unchanged for hydrations larger than the fiber saturation point.[2]

In earlier works[8,9] information on the cellulose fibril diameter and the orientation was gained from the SAXS spectra in an intermediate q region around $q \approx 0.3$ Å^{-1}. Data at smaller values of q were not interpreted, since they are influenced on the one side by the scattering of voids and on the other side by interference effects between the fibrils. The investigation of the same specimen at various degrees of hydration now enabled us to separate the contributions from pores and from the cell wall itself. The scattering intensity from the cell wall only, i.e. $I_x^{CW}(q)$, represents the Fourier transform of a two-dimensional cross-section perpendicular to the cellulose fibril direction of the S_2 cell-wall structure.

Concentrating first on the case of the native wood cell ($x > x_F$), it is now possible to derive more quantitative information on the arrangement of cellulose fibrils within the cell wall by comparing $G(q)$ to the prediction from a model structure. The simplest possibility is to describe the positions of the disks (representing the fibrils in cross-section) as being completely random besides the restriction that the disks cannot overlap. This is known as the hard-disk model whose structure function can be computed, e.g. by a Monte-Carlo procedure, as described in textbooks.[14−16] Such calculations actually yield the pair-correlation function $g(r)$ which is related to the structure function by the formula $G(q) = 1 + 2\pi\rho\int \mathrm{d}r\, rJ_0(qr)\, g(r)$. The interpretation of the pair-correlation function is that $g(r)$ is proportional to the probability of finding the center of a disk at a given position located at a distance r away from the center of another disk. The result for $g(r)$, and hence $G(q)$, depends only on one parameter, the packing density of the disks, given by $\rho = n\pi D^2/4$, where n is the number of disks per unit surface. To fit the data in Figure 7b, we computed the pair-correlation function $g(r)$ for several packing densities ρ and the best agreement was obtained for $\rho = 0.30$. A comparison with the measured structure function is shown in Figure 8a and a corresponding typical configuration of the hard-disk model in Figure 8b. The agreement between the data and the model is excellent given the error margins of the experiment. Hence, we conclude that $\rho = 0.30$ represents the packing density for the ECF's in the native cell wall of *P. abies* for hydrations above the fiber saturation point x_F.

To get an independent estimate for the packing density of cellulose fibrils in the cell wall layer S_2 of *P.*

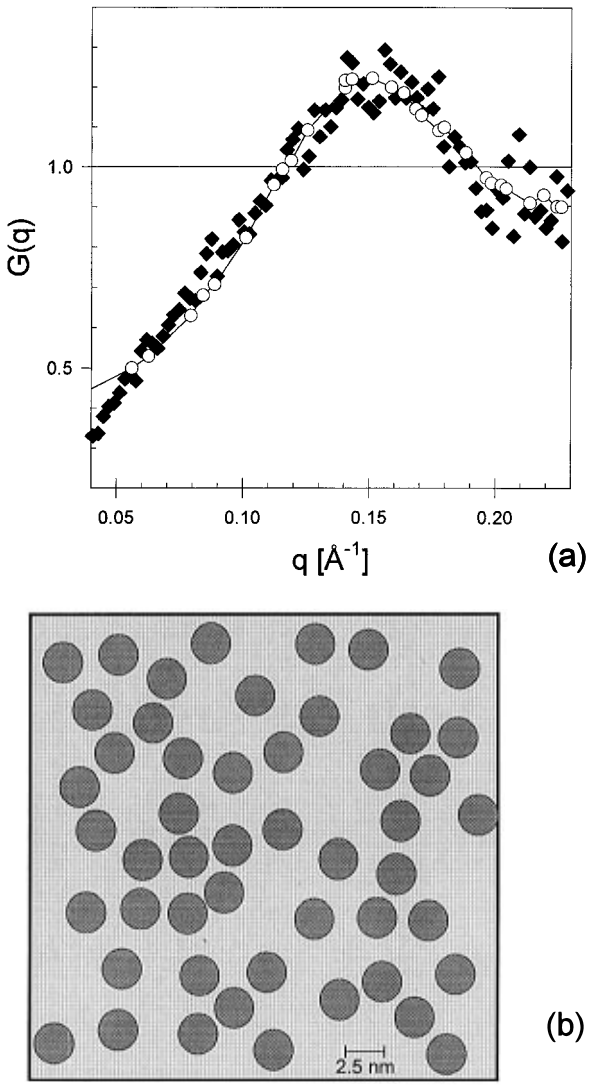

Figure 8. (a) Fit of the structure function $G(q)$ (diamonds) using Monte-Carlo simulations of a hard-sphere model (circles) with packing density $\rho = 0.30$. (b) Typical configuration of the hard-disk model with $\rho = 0.30$.

abies, one may take the composition of the dry layer to be $w_C = 58.5$ wt % cellulose, $w_P = 14.4$ wt % polyoses, and $w_L = 27.1$ w t% lignin, as determined by chemical analysis.[1,17,18] The densities of these components are $\rho_C = 1.60$ g cm^{-3} for cellulose, $\rho_P = 1.50$ g cm^{-3} for polyoses, and $\rho_L = 1.40$ g cm^{-3} for lignin, so that (for $x \le x_F$) the packing density $\rho = \rho(x)$ has the form

$$\rho(x) = \frac{w_C/\rho_C}{w_C/\rho_C + w_P/\rho_P + w_L/\rho_L + x/\rho_W}$$

where the numerator is the volume fraction of cellulose and the denominator the sum of the volume fractions of cellulose, polyoses, lignin, and water, respectively. This estimate assumes that the total volume of the cell wall is given by the sum of the volume fractions of the individual components, which is only a very rough estimate in the case of wood.[3] Moreover, the formula assumes that below the fiber saturation point, all water desorbs from the cell wall during drying. With these restrictions, the value estimated for $\rho(x = x_F)$ is 0.36, which is in reasonable agreement with the value obtained from SAXS, $\rho = 0.30$.

Consequently, Figure 8b can be considered as an adequate approximation for the arrangement of the

cellulose fibrils within the water-saturated cell-wall layer S_2. It is clearly visible that, while the fibril diameter is constant, some fibrils cluster together forming effectively larger aggregates, in agreement with earlier results.[8] Moreover, it should be noted that our X-ray scattering data do not exclude the possibility that individual cellulose molecules might join some of the adjacent fibrils, yielding an effectively more interconnected cellulose pattern than suggested by the well-separated circles in Figure 8b. Hence, it is difficult to say whether the fibrils are biosynthesized by direct means or by swelling and lignification of an originally lamellar cellulose structure,[19,20] as long as the result is a structure with a constant fibril diameter of 25 Å and a typical separation of about 40 Å. Also the actual shape of the fibril cross-section was assumed circular for simplicity. Different shapes, like square or hexagonal, were shown earlier to give practically the same scattering curve.[8] Hence, for fibrils with irregular shapes, the value of 25 Å may be considered as the diameter of the surface equivalent circle.

While the water-saturated structure, corresponding to the case of native wood, is well described by the picture in Figure 8, the structure was found to change dramatically below the fiber-saturation point (see Figure 2). Qualitatively, this could correspond to a decrease in the typical distance between the fibrils in Figure 8b. More detailed evaluations of these structural changes were not possible, since the scattering from pores became increasingly dominating at hydrations far below the fiber saturation point.

Acknowledgment. This work was supported by Fonds zur Förderung der wissenschaftlichen Forschung, FWF Project P10729-BIO.

References and Notes

(1) Fengel, D.; Wegener, G. *Wood Chemistry, Ultrastructure, Reactions*; De Gruyter: Berlin, New York, 1984.
(2) Bosshard, H. H. *Zur Biologie, Physik und Chemie des Holzes*; Holzkunde Band 2; Birkhäuser Verlag: Basel, 1984.
(3) Skaar, Ch. *Wood-water relations*; Springer series in wood science; Springer: Berlin, 1988.
(4) Frey-Wyssling, A. *The plant cell wall*, 3rd completely rev. ed.; Bornträger: Berlin u.a., 1976.
(5) Mörath, E. *Kolloidchem. Beih.* **1931**, *33*, 131.
(6) Kollmann, F. *Technologie des Holzes und der Holzwerkstoffe*; Springer-Verlag: Berlin, 1951; Vol. 1, Chapter 2.
(7) Trendelenberg R. *Das Holz als Rohstoff*; J. F. Lehmanns-Verlag: München, 1939.
(8) Jakob, H. F.; Fratzl, P.; Tschegg, S. E. *J. Struct. Biol.* **1994**, *113*, 13−22.
(9) Jakob, H. F.; Fengel, D.; Tschegg, S. E.; Fratzl, P. *Macromolecules* **1995**, *28*, 8782−8787.
(10) Fratzl, P. *J. Stat. Phys.* **1994**, *77*, 125−143.
(11) Guinier, A.; Fournet, G. *Small-Angle Scattering of X-rays*; Chapman & Hall: London, 1955.
(12) Glatter, O., Kratky O., Eds.; *Small Angle X-ray Scattering*; Academic Press: New York, 1982.
(13) Porod, G. *Kolloid.-Z.* **1951**, *124*, 83−114; **1952**, *125*, 51−57, 108−122.
(14) Binder, K. *Monte Carlo Methods in Statistical Physics*; Springer-Verlag: New York, 1979.
(15) Hansen, J. P.; McDonald, I. R. *Theory of simple liquids*; Academic Press: New York, 1976.
(16) Wood, W. W. *J. Chem. Phys.* **1970**, *52*, 729−741.
(17) Fengel, D. *Wood Sci. Technol.* **1969**, *3*, 203−217.
(18) Fengel, D. *Wood Sci. Technol.* **1970**, *4*, 15−35.
(19) Kerr, A. J.; Goring, D. A. I. *Cell. Chem. Technol.* **1975**, *9*, 563−573.
(20) Scallan, A. M. *Wood Sci.* **1974**, *6*, 266−271.

MA9605661